ANNALS OF TRANSPLANTATION

ORIGINAL PAPER

e-ISSN 2329-0358
© Ann Transplant, 2020; 25: e924272
DOI: 10.12659/AOT.924272

Received: 2020.03.14
Accepted: 2020.05.14
Available online: 2020.05.28
Published: 2020.07.10

Preparation of a Novel Transplant Material, Zirconium Oxide (ZrO_2) Nanotubes, and Characterizations Research

Authors' Contribution:
Study Design A
Data Collection B
Statistical Analysis C
Data Interpretation D
Manuscript Preparation E
Literature Search F
Funds Collection G

ABCDEFG 1 Chen Wang*
BCDEF 2 Yuchen Wang*
BCDF 3 Gengmin Zhang
BCD 3 Yanhui Chen
BCF 1 Xue Han
BCF 1 Li Liang
BC 1 Yiquan Xu
ABDE 2 Lulu Xu

1 Department of Stomatology, Eighth Medical Center, General Hospital of Chinese People's Liberation Army (PLA), Beijing, P.R. China
2 Department of Orthodontics, First Medical Center, General Hospital of Chinese People's Liberation Army (PLA), Beijing, P.R. China
3 Key Laboratory for the Physics and Chemistry of Nanodevices and Department of Electronics, Peking University, Beijing, P.R. China

* Chen Wang and Yuchen Wang contributed equally to this study

Corresponding Author: Chen Wang, e-mail: wangch1988@foxmail.com, Lulu Xu, e-mail: xululu1977@163.com

Source of support: This work was supported by the National Natural Science Foundation of China (Grant No. 81701018, 61671022, 8150030603) and grants from International Science and Technology Cooperation Projects (Grant No. 2015-TSYS-2028) and Clinical research support foundation of General Hospital of Chinese PLA (Grant No. 2017 FC-TSYS-3013)

Background: Zirconia is one of the most widely used ceramic materials for transplanting and treating caries. This study aimed to synthesize zirconium oxide (ZrO_2) nanotubes and evaluated their characteristics.

Material/Methods: Zr film was prepared using an ion plating method. Nanoarray film was constructed with anodizing. Photocatalytic properties of nnanotubes were assessed by evaluating decolorization of methyl orange. Elemental analysis and structural morphology for coatings were evaluated using x-ray analysis and scanning electron microscopy (SEM). Dimensions for layers were measured with SEM imaging. X-ray diffraction (XRD) was measured using Empyrean x-ray diffractometry.

Results: There were irregular cavities on the surface of ZrO_2 nanotubes undergoing anodizing of 30V. Anodizing voltage of 45 V (with regular nano-pore arrays and smooth nanotube walls) and anodic oxidation duration of 60 min (ZrO_2 nanotubes clearly formed atop ZrO_2-coated substrate surface) were the optimal condition for ZrO_2 nanotube formation. TEM illustrated tube length of ZrO_2 nanotubes was approximately 2.01 μm. Nanotube diameter was 51.06 nm, and wall thickness was 13 to 14 nm. Annealed nanotubes showed an obvious crystal diffraction pattern. TEM diffraction ring showed nanotube array without obvious transistor structure before annealing, but with good crystallinity post-annealing. Increased annealing temperatures result in enhanced intensity for the monoclinic phase (400–800°C). After annealing at 600°C, the decolorization effect of ZrO_2 nanotubes on methyl orange was better than that post-annealing at 400 and 800°C. ZrO_2 nanotubes demonstrated higher micro-shear bond strength.

Conclusions: Zirconium nanotubes were successfully synthesized and demonstrated good structural characteristics, which can be applied to transplanting and treating caries.

MeSH Keywords: **Biocompatible Materials • Dental Caries • Engineering • Nanotubes • Zirconium**

Full-text PDF: https://www.annalsoftransplantation.com/abstract/index/idArt/924272

Indexed in: [Science Citation Index Expanded] [Index Medicus/MEDLINE] [Chemical Abstracts] [Scopus]

Background

Caries are an oral disease with the highest incidence in human beings [1,2]. Serious defects in teeth and dentition caused by caries greatly damage the general health of patients, and even their mental health [3]. Zirconium (Zr), as a second-row transition metal, was first isolated in 824 and many organometallic or inorganic complexes of Zr have been discovered to date. Zr is characterized by mechanical strength, higher transparency to thermal neutrons, resistance against corrosion, and has been widely applied in surgical tools, dye pigments, lamp filaments, and ceramics [4]. Many materials contain Zr, which inevitably enter the environment, drinking water, and living organisms. Zr salts or complexes demonstrate high reactivity to the phosphodiester cleavage of the backbones for nucleic acid in weak acid or homogeneous solutions [5].

Zirconia is one of the most widely used and transplanted ceramic materials in treatment of caries [6]. It is also extensively used in manufacture of full crown, root pin, multiunit fixed bridge base crown, implants, and other restorations [7]. However, zirconia's composition makes it difficult to form sufficient mechanical and chemical adhesion between resin and zirconia ceramics [8,9]. In the dental microenvironment, which is influenced by complex factors, zirconia ceramic restorations are prone to complications such as reduction of retention force, loss of restorations, microleakage of bonding interface, and secondary caries of abutment teeth. The failure rate for 5-year bonding repair is 4.7 to 8.3 times that for glass matrix ceramic restoration [10,11]. Therefore, to improve the mechanical-chemical bonding strength of a zirconia-ceramic resin bonding interface, it is key to improve the clinical bonding effect of zirconia ceramic restorations and promote success with aesthetic restoration of dental caries.

Currently, research onsurface modification of zirconia ceramics mainly focuses on increasing surface roughness of zirconia ceramics by mechanical coarsening or chemical coating, both of which play a role in chemical activation. Although the bonding strength of zirconia ceramic resin has improved to a certain extent, the surface modification effect of zirconia is also unstable [1,12]. Moreover, there are also some problems with zirconia ceramic, such as reduction intif mechanical strength and lack of obvious or lasting chemical activation effects [1,12]. New technologies and theories are constantly changing the concept of surface modification of materials.

Given the issues with the structural characteristics and physical and chemical properties of zirconia ceramics, a high-strength inorganic non-metallic material has been investigated as an alternative. Use of the surface coating with this material has gradually expands to encompass biomimetic and functional dentistry. In recent years, biomimetic surface modification has been become a hot field, with the technology simulating the gecko sucker and other biological structures. Furthermore, the three-dimensional nanostructure coating with super adhesion has been successfully synthesized and constructed. Zirconia ceramic has been extensively used in regeneration of detal tissue, based on the biomimetic theory [13,14].

The three-dimensional (3D) structure of dental tissue also promotes adhesion [15]. A demineralized enamel column "honeycomb" array structure and collagen fiber mesh scaffold can be formed by etching the enamel and dentin, respectively. All of this provides 3D support for infiltration and inlay of resin on its surface, and significantly increase the contact area and chemical reaction binding site with resin. The 3D structure and resin bonding "mixed layer" also can be formed between the greases, resulting in considerable bonding strength considerable and stability [16].

Given the above bionic principles, if we could simulate the bonding mechanism of tooth tissue on the surface of zirconia ceramic and construct a bionic 3D scaffold structure, it would greatly improve the bonding effects of zirconia ceramic and resin, and provide a better bonding strategy for zirconia ceramic restoration. In view of the properties of zirconia ceramics, such as its high-strength inorganic non-metallic characteristics [17], this study simulated the bonding mechanism of enamel with the aim of synthesizing zirconium dioxide (ZrO_2). ZrO_2 has been proven effective for selective separation of anions from aqueous solutions, and ZrO_2-coated magnetic particles have been applied to trap adsorbents for analysis of phosphopeptides [18,19]. ZrO_2 also has physical, photocatalystic, and chemical inertness; good mechanical properties; and electrical characteristics, all which make it suitable for application as a catalyst and photocatalyst [20]. Nanowire array film coating on the surface of zirconia, based on the construction of 3D array structures, simulates the "honeycomb" of a demineralized enamel column. A new biomimetic bonding strategy using zirconia ceramic with a "mixed layer" of zirconia ceramic resin bonding was constructed using the 3D nanoarray. This study may improve success rates with zirconia ceramic prosthetics in clinical bonding repair. Moreover, it may also provide new ideas for further applications for incorporation of zirconia ceramic in biomimetic materials used for applications such as craniomaxillofacial reconstruction, tissue regeneration, and remineralization.

Material and Methods

Preparation of Zr micro-film by ion plating method

Preparation for the Zr micro-film was conducted as described in the previous study [21] with a few modifications. Briefly,

Indexed in: [Science Citation Index Expanded] [Index Medicus/MEDLINE] [Chemical Abstracts] [Scopus]

before coating, the high temperature sintered- and sandpaper-polished Zirconia ceramic specimens were cleaned with the Ar-ion back sputtering, under vacuum conditions of 9×10^{-4} Pa for 5 min (Ar^+, 99.99%, air pressure 3.0 Pa, flow rate 20 seem, power 50 W, bias 0.3 kV). Subsequently, the zirconia ceramic specimen with Zr film was subjected to continuous coating for 8 h, with ion plating parameters of background vacuum 2×10^{-3} Pa, coating temperature 200°C, working gas Ar, pressure of 0.8 Pa, voltage of 21 V and current 80 A.

Construction of nanotubes array by anodizing

In this study, the ion-plated, Zr film-coated zirconia ceramic sheet was used as anode and a platinum sheet was used as a counter electrode. Construction of primary nanotubes was performed as described in previous studies [21,22], with a few modifications. Electrode spacing was kept at 2 cm. In brief, the pure zirconium films on the substrates of zirconia ceramic were anodized in NH4F electrolytes (Sigma-Aldrich., St. Louis, Missouri, USA, 0.5 wt%) dissolved in glycerol (Sigma-Aldrich., 99 wt%) and a distilled-water solution mixture at ambient temperature. The zirconia ceramic plate coated with Zr film was anodized using a direct-current power supply (Model: E3641A, Agilent Tech., Palo-Alto, California, USA) for variable times, and 10 minutes and 60 minutes post-anodization in organic electrolyte under 30, 45, 60 V voltage and magnetic stirring. A film with primary ZrO_2 nanoarray structure then was obtained. Subsequently, heat treatment was conducted with a furnace, with administration of argon gas at different temperatures (at 400, 600 and 800°C), for 4 h with the heating and cooling rates of 3°C/min. The final ZrO_2 nanotube array then was obtained.

Photocatalytic properties of zirconia nanotubes

In this study, methyl orange solution was used as a photocatalytic degradation object. The nanotube on the surface of a ceramic chip prepared with a ZrO_2 nanotube was scraped off (about 20 mg), and nanotube powder was used as the decolorization and degradation catalyst. Zirconia nanotubes were put into 30 mL of methyl orange solution with a concentration of 20 mg/L (adjusted pH 4.5), and dispersed by magnetic stirring and ultrasound. A 30-W ultraviolet germicidal lamp (illumination 0.37 klux) was used as an ultraviolet light source, and held perpendicular to and 20 cm above the solution. The reaction time was 8 hours, and a sample was taken every 30 minutes. Absorbance of methyl orange at 465 nm was measured using BioPhotometerplus UV-Vis photometer (Eppendorf, Hamburg, Germany). The standard curve of absorbance was calculated by linear regression of concentration and absorbance. Fitting formula: A=0.0686c+0.0026. Calculation formula of degradation rate: $D=(c_0-c)/c_0\times100\%$.

Characterization and screening of ZrO_2 nano array films

Elemental analysis and structural morphology for coatings were evaluated with a high-resolution FESEM device (Model: FEI-Quanta 200F) equipped with an energy dispersive x-ray analyzer and a transmission electron microscope (TEM, model: JEOL Tem2010, Agilent Tech., Palo-Alto, California, USA). Dimensions for layers were measured with the SEM imaging. X-ray diffraction (XRD) was measured using an Empyrean X-ray diffractometer (PANalytical, Netherland), as described in a previous study [21]. X-ray photo-electron spectroscopy was analyzed with a professional spectrometer (Model: VG-ESCALab II, VG Sci. Ltd., UK), with the Al Kα excitation-source.

Bonding processes and micro-shear bond strength test

Bonding procedures and a microshear bond strength test were conducted using the approach previously described by our team [23]. In this section, the specimen stored in the distilled water treatment for 3 days at 37°C was assigned as the immediate specimen. Therefore, the associated microshear bond strength in untreated Zr was defined as "UNT-3d" and in ZrO_2 nanotubes coated Zr was defined as "ZrNT-3d". Correspondingly, the aging microshear bond strength in untreated Zr was defined as "UNT-aging" and in ZrO_2 nanotubes coated Zr was defined as "ZrNT-aging".

Statistical analysis

Data were presented as mean±SD and analyzed using SPSS software 20.0 (SPSS Inc., Chicago, Illinois, USA). The student's *t* test was used to analyze differences between two groups. $P<0.05$ was defined as statistical significance.

Results

SEM images undergoing different anodic oxidation duration

For the primary surface of the Zr-coated substrate (before anodic oxidation), which is fairly flat, nanograins were accumulated atop the substrate (Figure 1A). However, there were obvious variations in morphology of ZrO_2-coated substrate surface after anodic oxidation treatment (Figure 1B, 1C). Figure 1B is a SEM image of ZrO_2-coated specimens after 10 minutes of anodic oxidation, and Figure 1C shows the structure of ZrO_2-coated substrate surface after 60 minutes of anodic oxidation. As shown in Figure 1, with anodic oxidation for 10 minutes, the nanotubes began to form the ZrO_2 nano-tube, with micro-cracks and micro-pores on the ZrO_2-coated substrate surface. When the anodic oxidation duration was prolonged

Indexed in: [Science Citation Index Expanded] [Index Medicus/MEDLINE] [Chemical Abstracts] [Scopus]

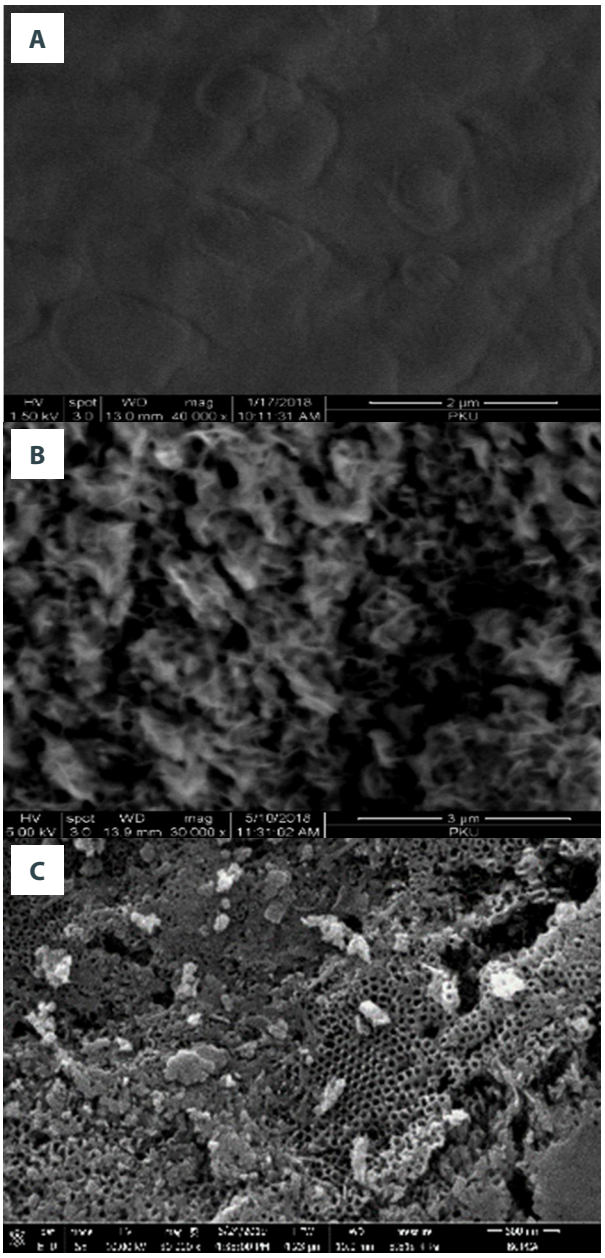

Figure 1. SEM images illustrating top-view for Zr-coated substrate (**A**) and ZrO_2-coated substrate at anodic oxidation duration for 10 min (**B**) and 30 min (**C**).

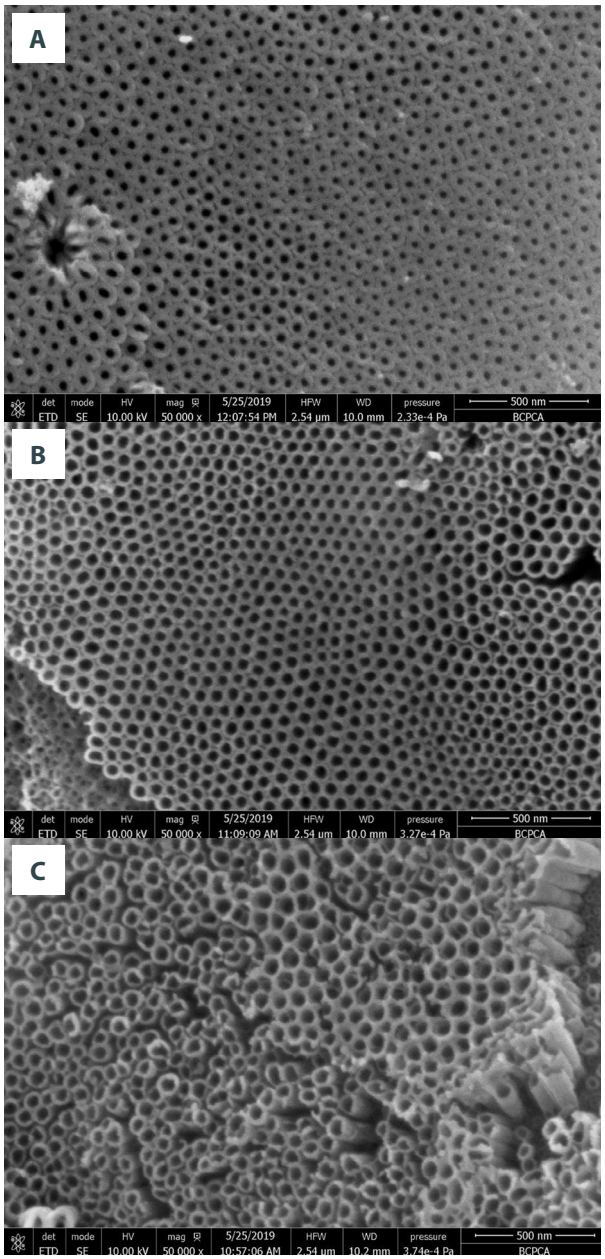

Figure 2. Effects of voltage on the morphology of the ZrO_2 Nanotube arrays. (**A**) Voltage of 30 V. (**B**) Voltage of 45 V. (**C**) Voltage of 60 V.

to 60 minutes (Figure 1B), ZrO_2 nanotubes clearly formed atop the ZrO_2-coated substrate surface (Figure 1C).

SEM images undergoing different anodizing voltages

Figure 1 shows SEM images of ZrO_2-coated substrates exposed to different voltages. Irregular cavities are apparent on the surface of ZrO_2 nanotubes undergoing 30 V anodization (Figure 2A). When the ZrO_2 was treated with 45 V of anodization, regular nanopore arrays with a diameter of 20 nm and a spacing of 100 nm formed on the surface of ZrO_2, with smooth nanotube walls (Figure 2B). Under the 45-V anodization, arrangement of the nanotube array was regular (Figure 2B). When the voltage was enhanced to 60 V, the nanotubes similar to in structure to a honeycomb formed on the surface of ZrO_2, with diameters of 80 to 120 nm (Figure 2C). However, compared to anodization at 45 V, the arrangement of nanotubes was irregular and some tube walls were broken (Figure 2C). Therefore, anodization at 45 V is considered to be the optimal voltage in this study.

Indexed in: [Science Citation Index Expanded] [Index Medicus/MEDLINE] [Chemical Abstracts] [Scopus]

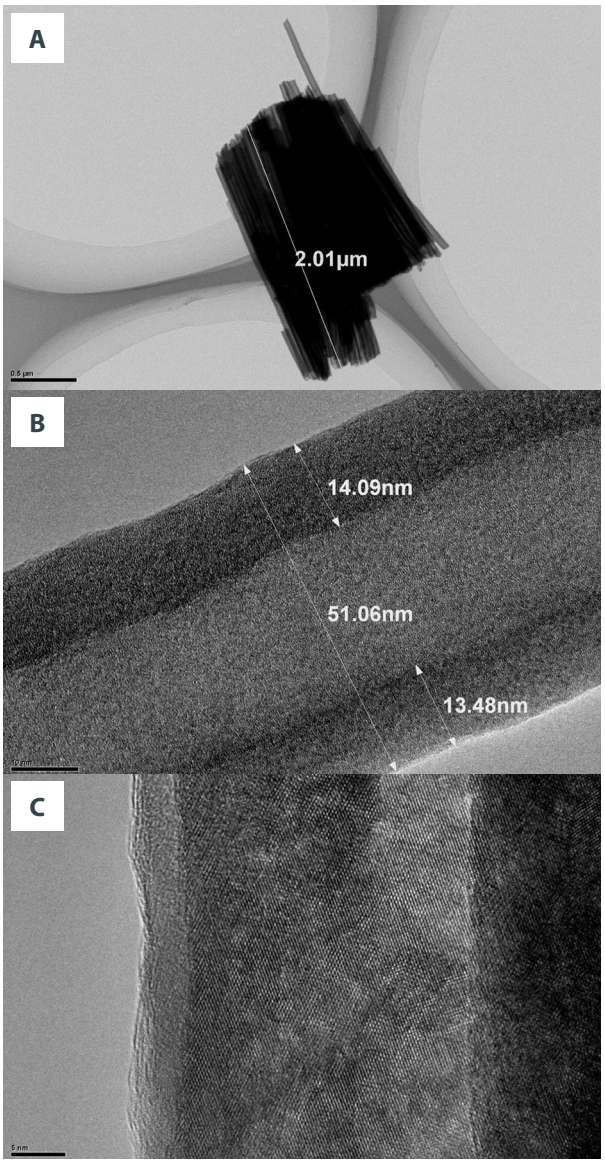

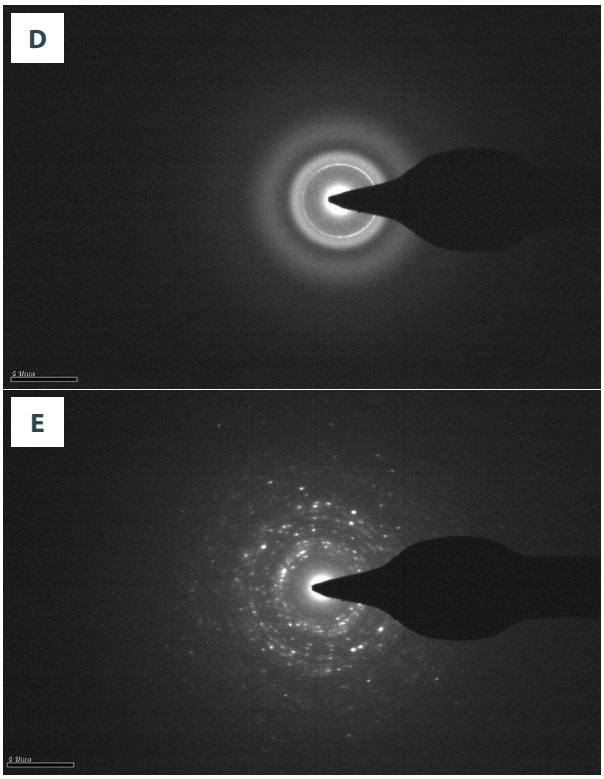

Figure 3. TEM images for nanotubes and their crystal structures. (**A**) General view for the ZrO_2 nanotubes. (**B**) TEM showed the wall structure of nanotubes before annealing. (**C**) TEM illustrating the obvious crystal diffraction patterns on the tube wall post the annealing. (**D**) TEM showed the diffraction ring before annealing. (**E**) TEM of annealed diffracted rings illustrating better crystallinity of nanotubes.

Combining the different anodic oxidation duration and different anodizing voltages, the anodizing voltage of 45 V and anodic oxidation duration of 60 minutes are the optimal conditions for ZrO_2 nano-tube formation, which were used in the following experiments.

TEM images for nanotubes and their crystal structure

TEM images of the nanotubes showed a tube length of about 2.01 μm (Figure 3A). Figure 3B shows TEM morphology of nanotubes before annealing, and there was no crystal diffraction pattern on the tube wall. The diameter of the nanotubes was about 51.06 nm, and thickness of the nanotube walls was about 13 to 14 nm (Figure 3B). At the same time, the annealed nanotubes showed an obvious crystal diffraction pattern (Figure 3C). Moreover, the TEM diffraction ring showed that the nanotube array had no obvious transistor structure before annealing (Figure 3D); however, the nanotube arrays had good crystallinity after annealing (Figure 3E).

XRD spectra undergoing different annealing temperatures

XRD patterns for Zr-coated substrate and ZrO_2 nanotube-coated substrates at different annealing temperatures (400, 600 and 800°C) were denoted inside the XRD graphs (Figure 4). Both Zr-coated substrate (Figure 4A) and ZrO_2 nanotube-coated substrates (Figure 4B) were amorphous prior to annealing. At the annealing temperature of 400°C, most diffraction peaks could be indexed as tetragonal-phase (Figure 4C), in which the main-peak for the tetragonal zirconia appeared at the 2^{-thera}=34°. At an annealing temperature of 600°C, intensity of peaks of both monoclinic phases and tetragonal phases were increased according to the more complete crystallization (Figure 4D). At the annealing temperature of 800°C, plenty of ZrO_2 Nano-tube arrays were of monoclinic phase and only a few ZrO_2 nanotube arrays were of tetragonal phase (Figure 4E).

Indexed in: [Science Citation Index Expanded] [Index Medicus/MEDLINE] [Chemical Abstracts] [Scopus]

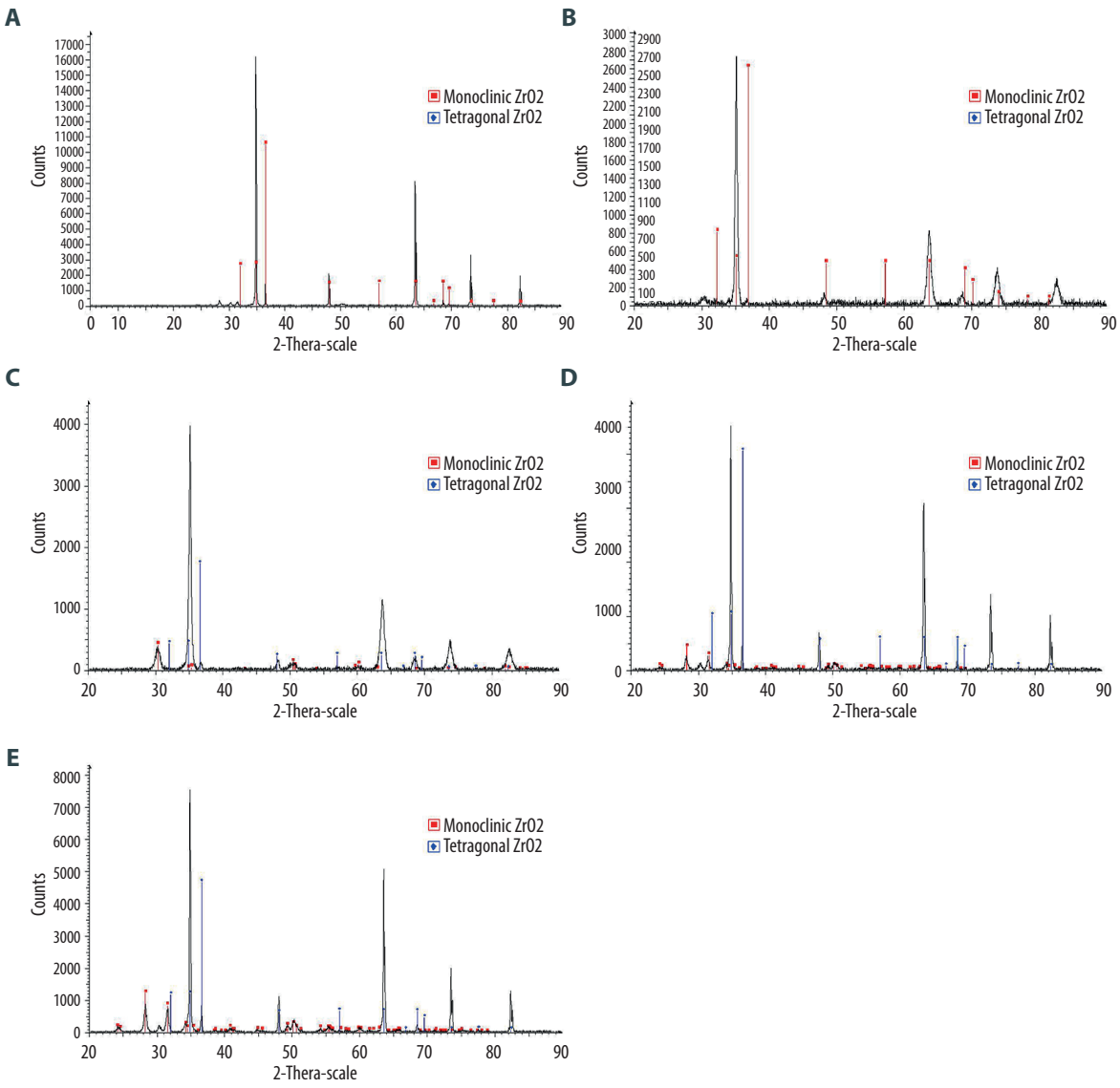

Figure 4. XRD spectra of the Zr coated (**A**), ZrO_2 coated substrate before annealing (**B**) and ZrO_2 coated substrates annealed at 400°C (**C**), 600°C (**D**) and 8000°C (**E**).

These results suggest that increased annealing temperatures result in enhanced intensity for monoclinic phase.

Photocatalytic properties of ZrO_2 nanotubes

In this study, photocatalytic properties of ZrO_2 nanotubes were expressed by the decolorization rate of methyl orange solution. The results showed that the decolorization effect of annealed ZrO_2 nanotubes was better than that of the annealed ones, and the photocatalytic performance was also improved (Figure 5). At the same time, after annealing at 600°C, the decolorization effect of ZrO_2 nanotubes on methyl orange was also better than that after annealing at 400°C and 800°C (Figure 5), showing the best photocatalytic performance.

ZrO_2 nanotubes demonstrated higher microshear bond strength

Microshear bond strengths in both the UNT-3d and the ZrNT-3d group were significantly higher compared to that in the UNT-aging and ZrNT-aging groups (Figure 6, $p<0.05$). Meanwhile, microshear bond strength was also higher significantly in the ZrO_2 nanotube groups (ZrNT-3d and ZrNT-aging group) compared to that in the untreated Zr groups (UNT-3d and UNT-aging group) (Figure 6, $p<0.05$).

Indexed in: [Science Citation Index Expanded] [Index Medicus/MEDLINE] [Chemical Abstracts] [Scopus]

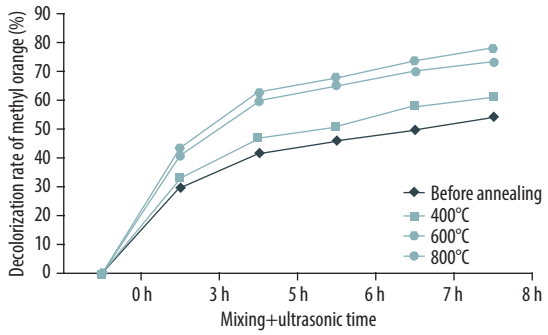

Figure 5. Photocatalytic properties of ZrO_2 nanotubes expressing by decolorization rate of methyl orange solution.

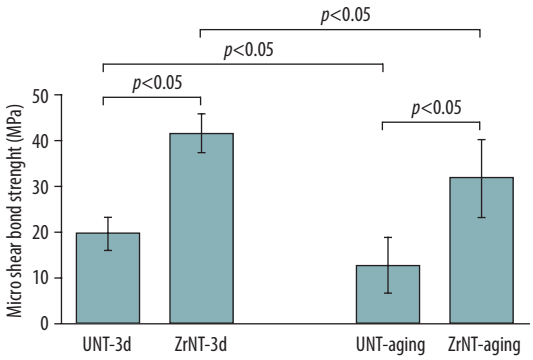

Figure 6. Micro shear bond strength findings in ZrO_2 nanotubes and untreated Zr groups.

Discussion

In recent years, ZrO_2 has been extensively investigated for potential applications related to its good chemical and/or physical characteristics, such as higher biocompatibility, lower electrical conductivity, and higher mechanical and/or thermal-resistance [24]. ZrO_2 materials mainly include nanotubes, nano-belts, nano-crystalline powder, thin films, nano-rods and nano-needles, all of which can be generated using various methods [21]. According to previous studies [25,26], the ZrO_2 nanotubes are synthesized by combining hydrothermal-treatment, template-assisted-deposition, and anodic-oxidation techniques.

In this study, synthesized ZrO_2 nanotubes were annealed at different temperatures and different anodizing voltages in administration of argon gas were investigated. Morphology of the ZrO_2 nanotubes undergoing the anodizing voltages of 30 V demonstrated irregular cavities and regular nano-pore arrays with a 20-nm diameter undergoing 45 V, with smooth nanotube walls. When voltage was enhanced to 60 V, nanotubes similar in structure to a honeycomb formed on the surface of ZrO_2, with diameters of 80 to 120 nm. However, compared to the anodizing voltage of 45 V, the arrangement of nanotubes was irregular and some tube walls were broken. Therefore, an anodizing voltage of 45 V was appropriate and optimal for synthesis of ZrO_2 nanotubes. An anodic oxidation duration of 60 minutes was the optimal condition for ZrO_2 nano-tube formation. After annealing at 400°C, 600°C and 800°C, the diameter of nanotubes reached 51.06 nm and thickness nanotubes reached 13 to 14 nm. Annealed nanotubes showed obvious crystal diffraction pattern. Given these observations as well as previous reports [21,27], it could be interpreted that ZrO_2 nanotubes post-annealing at 400°C, 600°C and 800°C are gradually compacted and become more and more brittle based on the nature of ceramics.

Given the TEM diffraction ring, we observed that the ZrO_2 nanotube array had no obvious crystalline structure before annealing. However, the ZrO_2 nano-tube arrays showed good crystallinity after annealing. ZrO_2 nanotubes, with their amorphous structure, can be used for medical implants and as photocatalysts and catalysts [28]. To convert their amorphous structure into a crystalline structure, it is critical to subject them to heat treatment, which is also applied to eliminate remaining fluoride.

Generally, there are three phases for Zr: tetragonal, monoclinic, and cubic [29]. The tetragonal and monoclinic phases are achieved at temperatures lower than 1000°C, and cubic phase is achieved at temperatures higher than 1000°C [30]. In the current study, we only focused on only the tetragonal and monoclinic phases. The pre-prepared Zr nanotubes and the annealed ZrO_2 nanotubes at different temperatures were illustrated as the XRD patterns. Both Zr-coated substrate and ZrO_2 nanotube-coated substrate were amorphous prior to annealing. At an annealing temperature of 400°C, most diffraction peaks could be indexed as tetragonal phase. At an annealing temperature of 600°C, intensity of peaks of both monoclinic and tetragonal phases were increased according to the more complete crystallization. At an annealing temperature of 800°C, plenty of ZrO_2 nano-tube arrays were of monoclinic phase and only a few ZrO_2 nanotube arrays were of tetragonal phase. These results suggest that increased annealing temperatures result in enhanced intensity in the monoclinic phase. Actually, transitions from the amorphous structure to the crystalline structure generally could be identified by resemblance between amorphous structures and the tetragonal phase. The previous study reported that there is a similarity in short-range order between the amorphous structure and tetragonal phase. Therefore, transformation from amorphous to tetragonal phase, as well as changes of structure, may occur when annealing temperature reaches 400°C [30].

Photocatalytic properties of ZrO_2 nanotubes for methyl orange degradation was also evaluated in this study. Under optimal reaction conditions, ZrO_2 nanotubes with monoclinic phase

Indexed in: [Science Citation Index Expanded] [Index Medicus/MEDLINE] [Chemical Abstracts] [Scopus]

illustrated a relatively higher methyl orange degradation rate compared to ZrO_2 nanotubes with tetragonal phase. The higher photocatalytic activity of the ZrO_2 nanotubes with monoclinic phase was attributed to the combined effects of several factors, including high crystallinity, small amounts of oxygen-deficient-zirconium oxide phase, high density for surface hydroxyl, and broad pore size distribution [31]. Moreover, we also proved that ZrO_2 nanotubes demonstrated higher microshear bond strength, which is critical for their application.

Conclusions

When voltage was enhanced to 60 V, regular hexagonal nanotubes were formed on surface of ZrO_2, with diameters between 80 and 120 nm and smooth nanotube walls. The tube length of ZrO_2 nanotubes was about 2.01 μm, with diameters of about 51.06 nm and thickness of 13 to 14 nm. Annealed ZrO_2 nanotubes showed an obvious crystal diffraction pattern and ZrO_2 nanotube arrays demonstrated good crystallinity afterannealing. Increased annealing temperatures resulted in enhanced intensity for the monoclinic phase (from 400°C to 800°C). After annealing at 600°C, the decolorization effect of ZrO_2 nanotubes on methyl orange was better than that after annealing at 400°C and 800°C, indicating the best photocatalytic performance. In summary, zirconium nanotubes were successfully synthesized and demonstrated good structural characteristics. Results of the current study may lead to improved bonding strength and clinical life for zirconia prosthetics, provide a theoretical basis for biomimetic bonding, and would be of great significance to improve the aesthetic treatment effect of teeth and dentition defects.

References:

1. Shen A, Bernabe E, Sabbah W: Severe dental caries is associated with incidence of thinness and overweight among preschool Chinese children. Acta Odontol Scand, 2020; 78: 203–9
2. Hu J, Jiang W, Lin X et al: Dental caries status and caries risk factors in students ages 12-14 years in Zhejiang, China. Med Sci Monit, 2018; 24: 3670–78
3. Drummond BK, Meldrum AM, Boyd D: Influence of dental care on children's oral health and wellbeing. Br Dent J, 2013; 214: E27
4. Shervedani RK, Bagherzadeh M: Elecrochemical impedance spectroscopy as a transduction method for electrochemical recognition of zirconium on gold electrode modified with hydroxamated self-assembled monolayer. Sensor Actuat B, 2009; 139: 657–64
5. Shervedani RK, Bagherzadeh M, Sabzyan H et al: One-impedance for one-concentration as an electrochemical method for determination of the trace zirconium ion. J Electroanal Chem, 2009; 633: 259–63
6. Rathmann F, Bomicke W, Rammelsberg P et al: Veneered zirconia inlay-retained fixed dental prostheses: 10-year results from a prospective clinical study. J Dent, 2017; 64: 68–72
7. Zhang X, Pei X, Pei X et al: Success and complication rates of root-filled teeth restored with Zirconia posts: A critical review. Int J Prosthodont, 2019; 32: 411–19
8. Ruyter EI, Vajeeston N, Knarvang T et al: A novel etching technique for surface treatment of ziconia ceramics to improve adhesion of resin-based luting cements. Acta Biomater Odontol Scand, 2017; 3: 36–46
9. Inokoshi M, Kameyama A, De Munck J et al: Durable bonding to mechanically and/or chemically pre-treated dental zirconia. J Dent, 2013; 41: 170–79
10. Bajraktarova-Valjakova E, Grozdanov A, Guguvcevski L et al: Acid etching as surface treatment method for luting of glass-ceramic restorations, part 1: Acids, application protocol and etching effectiveness. Open Access Maced J Med Sci, 2018; 6: 568–73
11. Aktas G, Burduroglu D, Guncu MB et al: Clinical survival of indirect, anterior surface-retained fiber-reinforced composite fixed dental prosthesis: Up to 3-year follow-up. Eur J Prosthodont Restor Dent, 2019; 27: 90–94
12. Traini T, Sorrentino R, Gherlone E et al: Fracture strength of Zirconia and alumina ceramic crowns supported by implants. J Oral Implantol, 2015; 41: 352–59
13. Huang CC, Narayanan R, Alapati S et al: Exosomes as biomimetic tools for stem cell differentiation: Applications in dental pulp tissue regeneration. Biomaterials, 2016; 111: 103–15
14. Cao Y, Mei ML, Li QL et al: Agarose hydrogel biomimetic mineralization model for the regeneration of enamel prismlike tissue. ACS Appl Mater Interfaces, 2014; 6: 410–20
15. Dejak B, Mlotkowski A: Three-dimensional finite element analysis of strength and adhesion of composite resin versus ceramic inlays in molars. J Prosthet Dent, 2008; 99: 131–40
16. Okamoto K, Ino T, Iwase N et al: Three-dimensional finite element analysis of stress distribution in composite resin cores with fiber posts of varying diameters. Dent Mater J, 2008; 27: 49–55
17. Bajraktarova-Valjakova E, Korunoska-Stevovska V, Kapusevska B et al: Contemporay dental ceramic materials, a review: Chemical composition, physical and mechanical properties, indications for Use. Open Access Maced J Med Sci, 2018; 6: 1742–55
18. Riahi F, Bagherzadeh M, Hadizadeh Z: Modification of Fe3N4 superparamagnetic nanoparticles with zirconium oxide, preparation, characterization and its application toward fluoride removal. RSC Adv, 2015; 5: 72058–68
19. Goudarzi MR, Bagherzadeh M, Fazilati M et al: Evaluation of antibacterial property of hydroxyapatite and zirconium oxide-modificated magnetic nanoparticles against *Staphylococcus aureus* and *Escherichia coli*. IET Nanobiotechol, 2019; 13: 449–55
20. Rostami-Vartooni A, Moradi-Saadatmand A, Bagherzadeh M et al: Green synthesis of $Ag/Fe_3O_4/ZrO_2$ nanocomposite using aqueous centaurea cyanus flower extract and its catalytic application for reduction of organic pollutants. Iran J Catal, 2019; 9: 27–35
21. Zalnezhad E, Hamouda AM, Jaworski J et al: From Zirconium nanograins to zirconia nanoneedles. Sci Rep, 2016; 6: 33282
22. Zalnezhadm E: Effect of structural evolution on mechanical properties of ZrO_2 coated Ti-6Al-7Nb-biomedicalapplication. Appl Surf Sci, 2016; 370: 32–39
23. Wang C, Niu LN, Wang YJ et al: Bonding of resin cement to zirconia with high pressure primer coating. PLoS One, 2014; 9: e101174
24. Zhang L, Han Y, Tan G: Hydroxyaptite nanorods patterned ZrO_2 bilayer coating on zirconium for the application of percutaneous implants. Colloids Surf B Biointerfaces, 2015; 127: 8–14
25. Dos Santos AF, Sandes de Lucena F, Sanches Banches AF et al: Incorporation of TiO_2 nanotubes in a polycrystalline zirconia: synthesis of nanotubes surface characterization, and bond strength. J Prosthet Dent, 2018; 120: 589–95
26. Gao QX: Photoluminescence properties of zirconia nanobelts with trace Sm3+ ions. Sci Adv Mater, 2012; 4: 327–31
27. Mayrhofer PH, Sonnleitner D, Bartosik M et al: Structural and mechanical evolution of reactively and non-reactively sputtered Zr-Al-N thin films during annealing. Surf Coat Technol, 2014; 244: 52–56
28. Yan H, Zgang M, Wei Q, Guo P: Theoretical study on tetragonal transition metal dinitrides from first principles calculations. Journal of Alloys and Compounds, 2013; 581: 508–14
29. Hatanaka GR, Polli GS, Fais LMS et al: Zirconia changes after grinding and regeneration firing. J Prosthet Dent, 2017; 118: 61–68
30. First RC, Heuer AH: Deformation twinning in single-crystal zirconia: A first report. J Am Ceram Soc, 1992; 75: 2302–3
31. Basahel SN, Ali TT, Mokhtar M et al: Influence of crystal structure of nanosized ZrO_2 on photocatalytic degradation of methyl orange. Nanoscale Res Lett, 2015; 10: 73

Indexed in: [Science Citation Index Expanded] [Index Medicus/MEDLINE] [Chemical Abstracts] [Scopus]